

# Quaternion Modeling and Observer-based Torque Compensation of an Aerial Manipulator <sup>★</sup>

J. U. Alvarez-Muñoz <sup>\*</sup> J. Escareno <sup>\*</sup> N. Marchand <sup>\*\*</sup>  
J. F. Guerrero-Castellanos <sup>\*\*\*</sup> T. Raharijaona <sup>\*\*\*\*</sup>  
M. Rakotondrabe <sup>†</sup>

<sup>\*</sup> *Institut Polytechnique des Sciences Avancées, FR-94200 Paris, France (e-mail: jonatan.alvarez, juan-antonio.escareno@ipsa.fr).*

<sup>\*\*</sup> *GIPSA-Lab, FR-38000 Grenoble, France, (e-mail: Nicolas.Marchand@inpg.fr)*

<sup>\*\*\*</sup> *Autonomous University of Puebla (BUAP), Faculty of Electronics, MX-72570 Puebla, Mexico (e-mail: fermi.guerrero@correo.buap.mx)*

<sup>\*\*\*\*</sup> *Aix Marseille Univ, CNRS, ISM, Marseille, France (e-mail: thibaut.raharijaona@univ-amu.fr)*

<sup>†</sup> *FEMTO-ST Institute, UMR CNRS-UFC/ENSMM/UTBM, Automatic Control and Micro-Mechatronic Department, 24, rue Alain Savary, Besancon, France (e-mail: mrakoton@femto-st.fr)*

---

**Abstract:** This paper proposes a simple solution regarding the stabilization of a quadcopter unmanned aerial vehicle endowed with a manipulator arm. The manipulator robot is attached below the rotors plane and this one induces torques producing stability issues. The present study deals with the stabilization of the full system (quadcopter and arm) by means of a set of nonlinear control techniques. First, a mathematical model is proposed for the system. Then, an attitude control, consisting on a bounded quaternion-based feedback allows the quadcopter attitude stabilization while compensating adverse torques from manipulator's motion. A simple-to-implement strategy is proposed to estimate the actual torque for compensation purposes. Then, the formulation of a nonlinear control, which drives the aerial vehicle to a desired position is presented. Both controls consist on saturation functions. Simulation results validate the proposed control strategy and compare the results with different manipulator torque estimations.

**Keywords:** Aerial Manipulation, Euler-Lagrange and Quaternion Modeling, Stochastic vs Deterministic State Estimation, Nonlinear Control

---

## 1. INTRODUCTION

Aerial manipulation has been an active area of research in recent times, mainly because the active tasking of Unmanned Aerial Vehicles (UAVs) increases the employability of these vehicles for various applications. For active task one would consider manipulation, grasping, transportation, etc.

Unlike fixed wings UAVs, that are incapable of driving their velocity to zero, VTOL (Vertical Take-Off and Landing) vehicles with four, six, or eight rotary wings (afterwards called multirotors) are ideally suited for aerial manipulation or grasping. However, there are many challenges in aerial grasping for these vehicles. The biggest challenge arises from their limited payload. While multiple robots can carry payloads with cables or grippers Mellinger et al. (2010), their end effectors and grippers have to be light weight themselves and capable of grasping complex shapes. Secondly, the dynamics of the robot is significantly altered by the addition of payloads. Indeed this is also an

attraction in assembly because aerial robots can use this to sense disturbance forces and moments, like in Mohammadi et al. (2016). Besides, for payload transport, it is necessary that the robots are able to estimate the inertia of the payload and adapt to it to improve tracking performance. Numerous approaches have been proposed to deal with such a problem. In Orsag et al. (2013a), a Lyapunov based model Reference Adaptive Control is used to stabilize a quadrotor with a multi degree of freedom (DOF) manipulator. Jimenez-Cano et al. (2013) presents a Newton-Euler approach to model and control a quadrotor through a Variable Parameter Integral Backstepping (VPIB). Kim et al. (2013) presents aerial manipulation using a quadrotor and a 2-DOF robot arm. The dynamic model of the whole system is obtained by the Euler-Lagrange formulation. Then, an adaptive sliding mode controller is designed. The effectiveness of the proposed method is experimentally showed by picking up and delivering an object. In Thomas et al. (2014) the problem is solved through an autonomous avian-inspired grasping method.

Finally, in Yuksel et al. (2016) a new class of aerial manipulator is presented, which is called protocentric. It

---

<sup>★</sup> This work was also supported by the CODE-TRACK project (ANR-17-CE05-0014-01).

consists on a PVTOL equipped with parallel manipulator arms attached to the Center Of Mass (CoM) of the aerial vehicle. A control law has been proposed for the case of rigid joints and validated through simulations.

The present paper proposes a bounded quaternion-based attitude controller tolerant to external disturbances via the observer-based compensation of the manipulator's torque. For this, a mathematical model considering the couplings between the aerial and manipulation subsystems is presented. Moreover, unlike the cited works, our design for attitude stabilization is based on quaternion formalism, avoiding singularities. Concerning the observer scheme, two approaches are presented to evaluate their effectiveness for the estimation of the manipulator's torque: a Luenberger observer and a linear Kalman filter.

With quaternion parametrization one proposes a constructive control law for the attitude and position stabilization. First, the design of a smooth almost globally asymptotically control law for attitude stabilization which takes into account the arm motion effects is introduced. Then, a globally asymptotically nonlinear controller for the translational dynamics is proposed. In general the control law is based in the usage of nested and sum of saturation functions. Simulation results validate the proposed strategy.

The paper is structured as follows. In section 2, the attitude model of the quadcopter with the manipulator arm is presented. Section 3 presents two strategies to estimate the angular position of each link in the robot manipulator. Then, the attitude and position control laws are formulated in section 4. Section 5 presents the simulation scenario and results. Finally, section 6 .

## 2. MATHEMATICAL MODELING

### 2.1 Unit quaternion and attitude kinematics

Consider two orthogonal right-handed coordinate frames: the body coordinate frame,  $B(x_b, y_b, z_b)$ , located at the center of mass of a rigid body and the inertial coordinate frame,  $N(x_n, y_n, z_n)$ , located at some point in the space (for instance, the earth NED frame). The rotation of the body frame  $B$  with respect to the fixed frame  $N$  is represented by the attitude matrix  $R \in SO(3) = \{R \in \mathbb{R}^{3 \times 3} : R^T R = I, \det R = 1\}$ .

The cross product between two vectors  $\xi, \varrho \in \mathbb{R}^3$  is represented by a matrix multiplication  $[\xi^\times] \varrho = \xi \times \varrho$ , where  $[\xi^\times]$  is the well known skew-symmetric matrix.

The  $n$ -dimensional unit sphere embedded in  $\mathbb{R}^{n+1}$  is denoted as  $\mathbb{S}^n = \{x \in \mathbb{R}^{n+1} : x^T x = 1\}$ . Members of  $SO(3)$  are often parameterized in terms of a rotation  $\beta \in \mathbb{R}$  about a fixed axis  $e_v \in \mathbb{S}^2$  by the map  $\mathcal{U} : \mathbb{R} \times \mathbb{S}^2 \rightarrow SO(3)$  defined as

$$\mathcal{U}(\beta, e_v) := I_3 + \sin(\beta)[e_v^\times] + (1 - \cos(\beta))[e_v^\times]^2 \quad (1)$$

Hence, a unit quaternion,  $q \in \mathbb{S}^3$ , is defined as

$$q := \begin{pmatrix} \cos \frac{\beta}{2} \\ e_v \sin \frac{\beta}{2} \end{pmatrix} = \begin{pmatrix} q_0 \\ q_v \end{pmatrix} \in \mathbb{S}^3 \quad (2)$$

where  $q_v = (q_1 \ q_2 \ q_3)^T \in \mathbb{R}^3$  and  $q_0 \in \mathbb{R}$  are known as the vector and scalar parts of the quaternion respectively. The quaternion  $q$  represents an element of  $SO(3)$  through the map  $\mathcal{R} : \mathbb{S}^3 \rightarrow SO(3)$  defined as

$$\mathcal{R} := I_3 + 2q_0[q_v^\times] + 2[q_v^\times]^2 \quad (3)$$

*Remark 2.1.*  $R = \mathcal{R}(q) = \mathcal{R}(-q)$  for each  $q \in \mathbb{S}^3$ , i.e. even quaternions  $q$  and  $-q$  represent the same physical attitude.

Denoting by  $\omega = (\omega_1 \ \omega_2 \ \omega_3)^T$  the angular velocity vector of the body coordinate frame,  $B$  relative to the inertial coordinate frame  $N$  expressed in  $B$ , the kinematics equation is given by

$$\begin{pmatrix} \dot{q}_0 \\ \dot{q}_v \end{pmatrix} = \frac{1}{2} \begin{pmatrix} -q_v^T \\ I_3 q_0 + [q_v^\times] \end{pmatrix} \omega = \frac{1}{2} \Xi(q) \omega \quad (4)$$

The attitude error is used to quantify mismatch between two attitudes. If  $q$  defines the current attitude quaternion and  $q_d$  the desired quaternion, i.e. the desired orientation, then the error quaternion that represents the attitude error between the current orientation and the desired one is given by

$$q_e := q_d^{-1} \otimes q = (q_{e_0} \ q_{e_v}^T)^T \quad (5)$$

where  $q^{-1}$  is the complementary rotation of the quaternion  $q$  which is given by  $q^{-1} := (q_0 \ -q_v^T)^T$  and  $\otimes$  denotes the quaternion multiplication, Shuster (1993).

### 2.2 Model of a quadcopter carrying a manipulator arm

The attitude dynamics and kinematics for the quadcopter have been reported in many works *e.g.* Guerrero-Castellanos et al. (2008); Alaimo et al. (2013). In these works it is considered that the quadcopter mass distribution is symmetric. However, the mass distribution of a quadcopter with a manipulator is no longer symmetrical and varies with the movement of the arm. Consider a quadcopter with a manipulator arm with  $n$  links attached to its lower part. If the dynamics of the arm is neglected, the attitude kinematics and dynamics is given by

$$\begin{pmatrix} \dot{q}_0 \\ \dot{q}_v \end{pmatrix} = \frac{1}{2} \Xi(q) \omega \quad (6)$$

$$J \dot{\omega} = -\omega^\times J \omega + \Gamma_T \quad (7)$$

where  $J \in \mathbb{R}^{3 \times 3}$  is the inertia matrix of the rigid body expressed in the body frame  $B$  and  $\Gamma_T \in \mathbb{R}^3$  is the vector of applied torques.  $\Gamma_T$  depends on the (control) couples generated by the actuators, the aerodynamic couples such as gyroscopic couples, the gravity gradient or, as in the case of the present work, the couple generated by the movement of a robot manipulator placed under the body. Here, only the control couples, gyroscopic couples and the couple generated by the manipulator is considered in the control design. Consequently,

$$\Gamma_T = \Gamma + \Gamma_{arm} + \Gamma_G \quad (8)$$

where  $\Gamma$  and  $\Gamma_G$  are the control torques and the vector of gyroscopic couples, Castillo et al. (2004), respectively. On the other hand, the vector  $\Gamma_{arm} = (\tau_1, \tau_2, \tau_3)^T$  is the torque exerted by the total propulsive force being applied at the quadcopter geometric center which is displaced from the center of mass.

The total torque exerted by the manipulator arm can be found from its dynamic model by:

$$M(\theta_{ai}) \ddot{\theta}_{ai} + C(\theta_{ai}, \dot{\theta}_{ai}) \dot{\theta}_{ai} + N(\theta_{ai}, \dot{\theta}_{ai}) = \tau_i \quad (9)$$

where  $\theta_{ai}$ ,  $\dot{\theta}_{ai}$  and  $\ddot{\theta}_{ai}$  are the angular position, velocity and acceleration vectors, respectively on each link,  $M \in \mathbb{R}^{3 \times 3}$  is the manipulator inertia matrix,  $C$  is a matrix containing

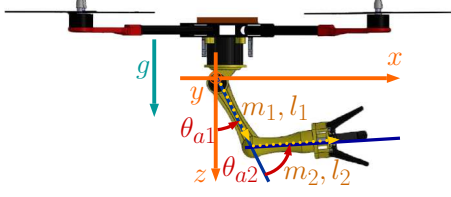


Figure 1. Manipulator arm with two degrees of freedom.

the Coriolis and centrifugal force terms,  $N$  includes gravity terms acting at the joints and  $\tau_i$  is the vector of the actuator torques.

To derive the dynamics of the system, the Lagrange equation is used

$$\frac{d}{dt} \frac{\partial \mathcal{L}}{\partial \dot{\theta}_{a_i}} - \frac{\partial \mathcal{L}}{\partial \theta_{a_i}} = \tau_i \quad (10)$$

$$\mathcal{L} = \mathcal{K} - \mathcal{U} \quad (11)$$

where  $\mathcal{K}$  and  $\mathcal{U}$  are the total kinetic and potential energy of the system and  $\tau_i$  represents the generalized force.

The kinetic energy can be computed from:

$$\mathcal{K} = \frac{1}{2} m_i v_i^T v_i + \frac{1}{2} I_i \theta_{a_i}^2 \quad (12)$$

where  $m_i$ ,  $v_i$  and  $I_i$  are the mass, the velocity vector and the inertia moments for every link in the manipulator, respectively.

Finally, the gravitational forces on the manipulator are computed from:

$$N(\theta_{a_i}, \dot{\theta}_{a_i}) = \frac{\partial U}{\partial \theta_{a_i}} \quad (13)$$

where  $U : \mathbb{R}^n \rightarrow \mathbb{R}$  is the potential energy of the manipulator. For the two link-manipulator under consideration here, the potential energy is given by

$$U(\theta_{a_i}) = U(\theta_{a_1}) + U(\theta_{a_2}) \quad (14)$$

Since each link has its own frame, the computed torque has a rotation matrix according to the axis in which the links are moving. Besides, the quadcopter rotation matrix is equally considered. Then, the computation of the manipulator's torque considering the dynamics is given by:

$$\Gamma_{arm} = \mathcal{R}(\tau_1 + R_1 \tau_2) \quad (15)$$

where  $\mathcal{R}$  was given by (3) and  $R_1$  is a rotation matrix on the  $y$  axis.

In this case, let consider the scheme in Fig. 1, which shows a 2-dof arm manipulator, where  $l_{c1}$  and  $l_{c2}$  are the distances from the respective joint axes to the center of mass of each link,  $l_1$  and  $l_2$  are the length of the links, and  $\theta_{a_i}$  measures the angular displacement in the  $x$  axis. Then, since servomotors are used as actuators for the manipulator arm, these can be considered as first order systems. For this, a parameter identification is performed. In general, the found system has the form:

$$\theta_{a_{i_m}} = \frac{K u(t) - a \dot{\theta}_{a_{i_m}}}{a} \quad (16)$$

where  $\theta_{a_{i_m}}$  and  $\dot{\theta}_{a_{i_m}}$  are the angular position and velocity of the servo,  $a$  is a time constant linked to the time response of the servo,  $K$  is the gain of the system and  $u(t)$  is the velocity input generated by the torque.

### 3. ESTIMATION STRATEGY AND TORQUE RECONSTRUCTION

This section presents two observers schemes to estimate joints angular displacements: a Luenberger state observer (LSO) and an augmented-state Kalman filter (ASKF). The estimation of joint angles in the manipulator arm is computed combining the data coming from the first order model of the manipulator actuators and the end effector position data tracked by a positioning system, since the first order model does not fully describe the behavior of the arm manipulator (non-modeled dynamics, actuators malfunction, etc.). Then, in order to know the manipulator links angular positions with respect to the base body (quadcopter), the inverse kinematics of the manipulator arm is used.

#### 3.1 Manipulator links Luenberger observer design

The objective of the observer is to estimate the angular positions and velocities on the arm manipulator, using the expression in (16).

A positioning system is used to obtain the end-effector position information and then, the inverse kinematics is applied to know the angle on each link. With this in consideration, the expression that describes a link angle is given by:

$$\theta_{aV} = \theta_a + \mu_V \quad (17)$$

where  $\theta_{aV}$  is the estimated angle computed with the positioning system and the inverse kinematics,  $\theta_a$  is the real angle and  $\mu_V$  is a noise of minimal value.

On the other hand, the observer allows the computation of the angular velocity. The expressions that represent the observer are given by:

$$\dot{\hat{\theta}}_\delta = a \hat{\theta}_\delta + K u_\delta + L(\theta_{aV} - \hat{\theta}) \quad (18)$$

$$\hat{\theta} = \hat{\theta}_V \quad (19)$$

where  $\hat{\theta}_\delta$  is the estimated angle on a link in the manipulator,  $a$  and  $K$  are parameters of the first order system previously presented and  $L$  is a positive tuning parameter.

#### 3.2 Augmented-state Kalman Filter

An augmented-state discrete linear Kalman filter (ASLKF) is designed regarding the estimation of the disturbances arising during the arm's planar joint displacement. The disturbed nominal model (16) is extended to include the velocity couplings between the aerial robot and the robotic arm

$$\dot{\theta}_{a_{i_m}} = -a \theta_{a_{i_m}} + b_i u_i(t) + \rho(t)_i \quad (20)$$

where  $\rho(t)$  corresponds to external disturbances (e.g. wind gusts), and whose dynamics is considered as

$$\dot{\rho} \approx 0 \quad (21)$$

Thus, it is possible to rewrite (20) and (21) into state-space representation

$$\begin{pmatrix} \dot{\theta}_{a_{i_m}} \\ \dot{\rho}_i \end{pmatrix} = \begin{pmatrix} -a_i & \rho_i \\ 0 & 0 \end{pmatrix} \begin{pmatrix} \theta_{a_{i_m}} \\ \rho_i \end{pmatrix} + \begin{pmatrix} k_i \\ 0 \end{pmatrix} u(t) \quad (22)$$

The Linear Kalman Filter (LKF) is derived from a continuous system

$$\begin{aligned} \dot{x}(t) &= Ax(t) + Bu(t) + P\rho + M\alpha(t) \\ y(t) &= Cx(t) + \beta(t) \end{aligned} \quad (23)$$

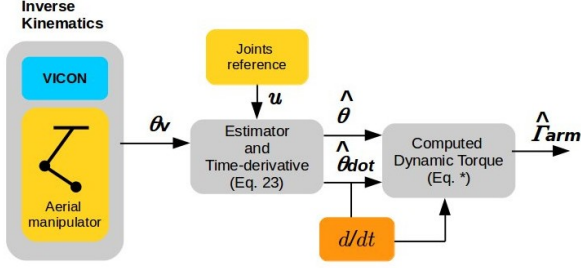


Figure 2. Observer-based manipulator's torque reconstruction

that considers that the pair  $AC$  verifies the controllability property. The signals  $\alpha$  (unmodeled dynamics and parametric uncertainties) and  $\beta$  (sensors noise) stand for a white Gaussian random process with zero-mean ( $E[\alpha(t)] = 0$ ) and  $E[\beta(t)] = 0$ ) with constant power spectral density (PSD)  $W(t)$  and  $V(t)$  defining respectively, the process covariance matrix,

$$Q = E[\alpha(t)\alpha(t+\tau)^T] = W\Delta(\tau) \quad (24)$$

, and the sensor covariance matrix,

$$R = E[\beta(t)\beta(t+\tau)^T] = V\Delta(\tau) \quad (25)$$

It is also assumed that both stochastic processes are not correlated, i.e.

$$E[\alpha(t)\beta(t)^T] = 0 \quad (26)$$

Including the disturbance as state the transition matrix is augmented and the state-space equations are written as

$$\dot{X}^e(t) = \mathcal{A}X^e(t) + \mathcal{B}(u_i) + \mathcal{M}\alpha_i \quad (27)$$

$$Y^e(t) = \mathcal{C}X^e(t) + \beta_i \quad (28)$$

In the previous regard, let us modify the extended model of the servomotor (22)

$$\begin{pmatrix} \dot{\theta}_{ai_m} \\ \dot{\rho}_i \end{pmatrix} = \begin{pmatrix} -a_i & \rho_i \\ 0 & 0 \end{pmatrix} \begin{pmatrix} \theta_{ai_m} \\ \rho_i \end{pmatrix} + \begin{pmatrix} k_i \\ 0 \end{pmatrix} u(t) + \begin{pmatrix} 1 & 0 \\ 0 & 1 \end{pmatrix} \begin{pmatrix} \alpha_\theta \\ \alpha_\rho \end{pmatrix} \quad (29)$$

Finally, the classical linear Kalman filter is applied to (29).

### 3.3 Torque Reconstruction

Based on the information provided by the LSO and ASKF presented before, it is possible to compute the manipulator torque from the equation (15) and use this term as  $\Gamma_{arm}$  into the attitude control law (32).

## 4. ATTITUDE AND POSITION CONTROL

### 4.1 Attitude Control: Problem statement

The objective is to design a control law which drives the quadcopter carrying the manipulator arm to attitude stabilization. Let  $q_d$  denotes the constant quadcopter stabilization orientation, then the control objective is described by the following asymptotic conditions

$$q \rightarrow [\pm 1 \ 0 \ 0 \ 0]^T, \quad \omega \rightarrow 0 \text{ as } t \rightarrow \infty \quad (30)$$

Furthermore, it is known that actuator saturation reduces the benefits of the feedback. Then, besides the asymptotic stability, the control law also takes into account the physical constraints of the system in order to apply only feasible control signals to the actuators.

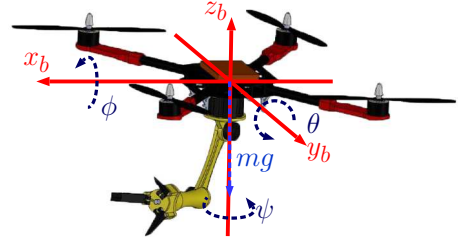


Figure 3. Schematic configuration of a quadrotor carrying a manipulator arm.

### 4.2 Attitude control with manipulator arm

In this subsection, a control law that stabilizes the system described by (6) and (7) is proposed. The goal is to design a control torque that is bounded.

*Definition 4.1.* Given a positive constant  $M$ , a continuous, nondecreasing function  $\sigma_M : \mathbb{R} \rightarrow \mathbb{R}$  is defined by

$$\begin{aligned} (1) \sigma_M &= s \text{ if } |s| < M; \\ (2) \sigma_M &= \text{sign}(s)M \text{ elsewhere.} \end{aligned} \quad (31)$$

Note that the components of  $\Gamma_{arm_i}$  are always bounded, i.e.  $|\Gamma_{arm_i}| < \delta_i$ . Then, one has the following result.

*Theorem 4.2.* Consider a rigid body rotational dynamics described by (6) and (7) with the following bounded control inputs  $\Gamma = (\Gamma_1 \ \Gamma_2 \ \Gamma_3)^T$  such that

$$\Gamma_i = -\sigma_{M_{i2}}(\Gamma_{arm_i} + \sigma_{M_{i1}}(\lambda_i[\omega_i + \rho_i q_i])) \quad (32)$$

with  $i \in \{1, 2, 3\}$  and where  $\sigma_{M_{i1}}$  and  $\sigma_{M_{i2}}$  are saturation functions. Assuming  $\delta_i < M_{i2} - M_{i1}$  and  $M_{i1} \geq 3\lambda_i\rho_i$ .  $\lambda_i$  and  $\rho_i$  are positive parameters. Then the inputs (32) asymptotically stabilize the rigid body to the origin  $(1 \ 0^T \ 0^T)^T$  (i.e.  $q_0 = 1, q_v = 0$  and  $\omega = 0$ ) with a domain of attraction equal to  $\mathbb{S}^3 \times \mathbb{R}^3 \setminus (-1 \ 0^T \ 0^T)^T$ .

### 4.3 Position control: Problem statement

The objective is to design a control law which stabilizes the quadcopter to a desired position. Once the control law has stabilized the attitude of the system, the position control law should stabilize the quadcopter to a desired position,  $\lim_{t \rightarrow \infty} (\mathbf{p}, \mathbf{v}) = (\mathbf{p}_d, \mathbf{0})$ .

### 4.4 Position stabilization strategy

The schematic representation of a quadcopter carrying a manipulator arm can be seen in Fig. 3, where the inertial reference frame  $N(x_n, y_n, z_n)$ , the body reference frame  $B(x_b, y_b, z_b)$ , the force  $u$  (thrust) and the weight vector  $mg$  are depicted. The dynamics of the whole system is obtained with the Newton-Euler formalism and the kinematics is represented using the quaternions formalism, given by

$$\Sigma_T : \begin{cases} \dot{\mathbf{p}} = \mathbf{v} \\ m_T \dot{\mathbf{v}} = -m_T \mathbf{g} + R \begin{pmatrix} 0 \\ 0 \\ u \end{pmatrix} \end{cases} \quad (33)$$

$$\Sigma_O : \begin{cases} \dot{q} = \frac{1}{2} \Xi(q) \omega \\ J \dot{\omega} = -\omega \times J \omega + \Gamma_T \end{cases} \quad (34)$$

where  $\mathbf{p}$  and  $\mathbf{v}$  are linear position and velocity vectors,  $m_T$  is the total mass of the system,  $\mathbf{g}$  is the gravity,  $R$  is the rotation matrix, given in (3).

Note that the rotation matrix  $R$  can also be given in function of the Euler angles, given in Castillo et al. (2004).

Now, assume that using the control law (32) one can stabilize the yaw dynamics, that is  $\psi = 0$ , then after a sufficiently long time, system (33) becomes:

$$\begin{pmatrix} \dot{p}_x \\ \dot{p}_y \\ \dot{p}_z \end{pmatrix} = \begin{pmatrix} v_x \\ v_y \\ v_z \end{pmatrix}, \quad (35)$$

$$\begin{pmatrix} \dot{v}_x \\ \dot{v}_y \\ \dot{v}_z \end{pmatrix} = \begin{pmatrix} -\frac{u}{m_T} \sin \theta \\ \frac{u}{m_T} \sin \phi \cos \theta \\ \frac{u}{m_T} \cos \phi \cos \theta - g \end{pmatrix} \quad (36)$$

With an appropriate choice of the target configuration, it will be possible to transform (35)-(36) into three independent linear triple integrators. For this, take

$$\begin{aligned} \phi_d &:= \arctan\left(\frac{r_2}{r_3 + g}\right), \\ \theta_d &:= \arcsin\left(\frac{-r_1}{\sqrt{r_1^2 + r_2^2 + (r_3 + g)^2}}\right) \end{aligned} \quad (37)$$

where  $r_1$ ,  $r_2$  and  $r_3$  will be defined after. Then, choose as positive thrust the input control

$$u = m_T \sqrt{r_1^2 + r_2^2 + (r_3 + g)^2} \quad (38)$$

By taking (35) and (36), it follows:

$$\Sigma_x : \begin{cases} \dot{p}_1 = p_2 \\ \dot{p}_2 = p_3 \\ \dot{p}_3 = r_1 \end{cases} \quad \Sigma_y : \begin{cases} \dot{p}_4 = p_5 \\ \dot{p}_5 = p_6 \\ \dot{p}_6 = r_2 \end{cases} \quad \Sigma_z : \begin{cases} \dot{p}_7 = p_8 \\ \dot{p}_8 = p_9 \\ \dot{p}_9 = r_3 \end{cases} \quad (39)$$

Note that  $u$  will be always positive, and  $u \geq mg$ , in order to compensate the system's weight.

Since the chains of integrators given in (39) have the same form, a control law can be proposed as in Cruz-José et al. (2012), and can be established by the next theorem:

*Theorem 4.3.* Consider the quadcopter translational dynamics expressed in (35-36). Then, the thrust input  $u$ , with control laws  $r_1, r_2, r_3$  as in (40), where  $\sigma_{M_1}(\cdot)$  is defined in (31) with  $M_1 = 1$  and  $\varsigma_i$  are given by (41),  $a_{(1,2,3)}, b_{(1,2,3)}, c_{(1,2,3)} > 0$  tuning parameters.

$$\begin{aligned} r_1 &:= -\varsigma_1 \{a_3 \sigma_{M_1}[\frac{1}{\varsigma_1}(a_2 p_1 + p_2 + p_3)] \\ &\quad + a_2 \sigma_{M_1}[\frac{1}{\varsigma_1}(a_1 p_2 + p_3)] + a_1 \sigma_{M_1}[\frac{1}{\varsigma_1}(p_3)]\}, \\ r_2 &:= -\varsigma_2 \{b_3 \sigma_{M_1}[\frac{1}{\varsigma_1}(b_2 p_4 + p_5 + p_6)] \\ &\quad + b_2 \sigma_{M_1}[\frac{1}{\varsigma_2}(b_1 p_5 + p_6)] + b_1 \sigma_{M_1}[\frac{1}{\varsigma_2}(p_6)]\}, \\ r_3 &:= -\varsigma_3 \{c_3 \sigma_{M_1}[\frac{1}{\varsigma_1}(c_2 p_7 + p_8 + p_9)] \\ &\quad + c_2 \sigma_{M_1}[\frac{1}{\varsigma_3}(c_1 p_8 + p_9)] + c_1 \sigma_{M_1}[\frac{1}{\varsigma_3}(p_9)]\} \end{aligned} \quad (40)$$

$$\begin{aligned} \varsigma_1 &= \bar{r}_1 / (a_1 + a_2 + a_3), \\ \varsigma_2 &= \bar{r}_2 / (b_1 + b_2 + b_3), \\ \varsigma_3 &= \bar{r}_3 / (c_1 + c_2 + c_3) \end{aligned} \quad (41)$$

The proof of this Theorem is not presented here, but it can be derived from the seminal work of Marchand and Hably (2005), Teel (1992) and Johnson and Kannan (2003).

*Remark 4.4.* In the above Theorem, the stabilization goal is the origin. In the case where the asymptotic condition is different from the origin, the variables  $p_2, p_5, p_8$  should be replaced in the control law (40) by  $e_1 = p_2 - p_x^d$ ,  $e_2 = p_5 - p_y^d$ ,  $e_3 = p_8 - p_z^d$ , respectively. In this case  $p_x^d, p_y^d, p_z^d$  represent the desired position in the space.

## 5. SIMULATION RESULTS

This section presents numerical results to show the effectiveness of the proposed control-estimation strategy of a quadrotor having a 2-DOF robotic manipulator. The simulation model features the parameters depicted by the Table 1.

Table 1.

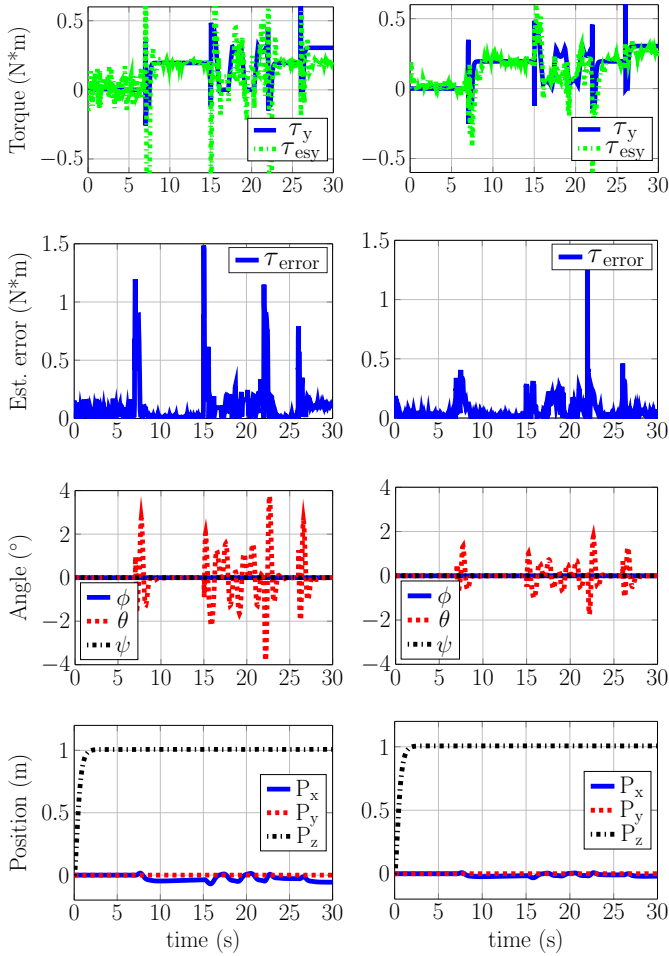
System	Description	Value	Units
Quadcopter	Mass (m)	590	g
	Distance (d)	25	cm
	Inertial moment $x$ ( $J_\phi$ )	0.0039	$Kg \cdot m^2$
	Inertial moment $y$ ( $J_\theta$ )	0.0039	$Kg \cdot m^2$
Manipulator	Inertial moment $z$ ( $J_\psi$ )	0.0073	$Kg \cdot m^2$
	Mass $m_a$	160	g
	Length links $l_1$ and $l_2$	12	cm

### 5.1 Simulation scenario

A set of simulations were carried out in order to compare the performance of the proposed control-estimation strategies, scenario 1 and scenario 2, respectively. For the attitude control law (32) and the position control law given in (40), where  $\max|\Gamma_{armi}| = 0.65Nm$  and  $\delta_i = 0.1$ , the next parameters values are proposed:  $M_{11,21,31} = 1.5$ ,  $M_{12,22} = 1$ ,  $M_{32} = 0.8$ ,  $\lambda_{1,2} = 0.035$ ,  $\lambda_3 = 0.033$ ,  $\rho_{1,2} = 10.5$  and  $\rho_3 = 11$ . For the control (40),  $a_1 = b_1 = 5.2$ ,  $c_1 = 0.45$ ,  $a_2 = b_2 = 2.3$ ,  $c_2 = 2$ ,  $a_3 = b_3 = 0.1$ ,  $c_3 = 0.05$  and  $\bar{r}_{1,2,3} = 6$ . The simulations consists on two parts. First, the links of the manipulator arm are initialized to  $\theta_{ai} = (0^\circ \ 0^\circ)^T$  and the quadrotor is driven to the position  $\mathbf{p}_d = (0 \ 0 \ 1)^T$ , then, at time 7s the links change to  $\theta_{ai} = (45^\circ \ 45^\circ)^T$ , at 15s the manipulator links perform a signal tracking given by  $\theta_{ai} = ((30 \sin(2t) + 40)^\circ \ (4 \sin(1.5t) + 5)^\circ)^T$ , at 22s the angles change to  $\theta_{ai} = (0^\circ \ 90^\circ)^T$ . Finally, at time 26s a constant disturbance is exerted to the manipulator and the simulation finishes.

Fig. 4 shows the simulation results using the two estimation strategies: Luenberger observer and Kalman filter. From top to bottom it shows the real and the estimated manipulator torques, the torque errors, and the angular and linear positions of the aerial robot during the simulation.

A general comparison can be made from the obtained results. First, the Luenberger observer or the Kalman filter, estimate the torque generated by the manipulator arm, then this estimation is used by the attitude control law as a feed-forward term in order to compensate the perturbation. From the results, the Kalman filter allows a better torque estimation. Even more, the Kalman filter is able to estimate the external constant disturbance. Consequently,



(a) Results using Luenberger observer. (b) Results using Kalman filter.

Figure 4. General behavior of the system during the simulation.

the computed control signals allow a better orientation stabilization and then, the non-desired displacement along the 3d space is reduced.

## 6. CONCLUSIONS

In this paper, a novel model for a quadcopter carrying a manipulator arm was proposed. Besides, a control law was designed to asymptotically stabilize the attitude and position of the system. Moreover, this work has presented two strategies for aiding the solution through the design of a Luenberger observer or a Kalman filter to develop a feed-forward term which allows the estimation of the moments and torques exerted by the manipulator. Simulation results show the effectiveness of the proposed estimation-control strategy face to the disturbances coming from the manipulator. With the use of two strategies, a comparison was performed, showing that the usage of the Kalman filter allows a better stabilization of the system. As a future work, experimental torque and mass estimations for picking up and delivery an object will be pursued.

## REFERENCES

Alaimo, A., Artale, V., Milazzo, C., Ricciardello, A., and Trefiletti, L. (2013). Mathematical modeling and control

- of a hexacopter. In *2013 International Conference on Unmanned Aircraft Systems (ICUAS)*, 1043–1050.
- Castillo, P., Dzul, A., and Lozano, R. (2004). Real-time stabilization and tracking of a four rotor mini rotorcraft. In *IEEE Transactions on Control Systems Technology*, volume 12, 510–516.
- Cruz-José, R., Guerrero-Castellanos, J.F., Guerrero-Sánchez, W.F., and Oliveros-Oliveros, J.J. (2012). Estabilización global de mini naves aéreas tipo vtol. In *Congreso Nacional de Control Automático*. Campeche, México.
- Guerrero-Castellanos, J.F., Marchand, N., Lesecq, S., and Delamare, J. (2008). Bounded attitude stabilization: Real-time application on four-rotor mini-helicopter. In *17th IFAC World Congress*. Seoul, Korea.
- Jimenez-Cano, A., Martin, J., Heredia, G., Ollero, A., and Cano, R. (2013). Control of an aerial robot with multi-link arm for assembly tasks. In *2013 IEEE International Conference on Robotics and Automation*, 4916–4921.
- Johnson, E.N. and Kannan, S.K. (2003). Nested saturation with guaranteed real poles. In *American Control Conference, 2003. Proceedings of the 2003*, volume 1, 497–502. IEEE.
- Kim, S., Choi, S., and Kim, H.J. (2013). Aerial manipulation using a quadrotor with a two dof robotic arm. In *2013 IEEE/RSJ International Conference on Intelligent Robots and Systems*, 4990–4995. doi: 10.1109/IROS.2013.6697077.
- Marchand, N. and Hably, A. (2005). Global stabilization of multiple integrators with bounded controls. *Automatica*, 41(12), 2147–2152.
- Mellinger, D., Shomin, M., and Kumar, V. (2010). Cooperative grasping and transport using multiple quadrotors. In *International Symposium on Distributed Autonomous Systems*. Lausanne, Switzerland.
- Mohammadi, M., Franchi, A., Barcelli, D., and Praticchizzo, D. (2016). Cooperative aerial tele-manipulation with haptic feedback. In *2016 IEEE/RSJ International Conference on Intelligent Robots and Systems (IROS)*, 5092–5098.
- Orsag, M., Korpela, C., Bogdan, S., and Oh, P. (2013a). Lyapunov based model reference adaptive control for aerial manipulation. In *2013 International Conference on Unmanned Aircraft Systems (ICUAS)*, 966–973.
- Shuster, M.D. (1993). A survey of attitude representations. *Journal of the Astronautical Sciences*, 41, 439–517.
- Teel, A.R. (1992). Global stabilization and restricted tracking for multiple integrators with bounded controls. *Systems & control letters*, 18(3), 165–171.
- Thomas, J., Loianno, G., Sreenath, K., and Kumar, V. (2014). Toward image based visual servoing for aerial grasping and perching. In *Robotics and Automation (ICRA), 2014 IEEE International Conference on*, 2113–2118. IEEE.
- Yuksel, B., Buondonno, G., and Franchi, A. (2016). Differential flatness and control of protocentric aerial manipulators with any number of arms and mixed rigid-/elastic-joints. In *2016 IEEE/RSJ International Conference on Intelligent Robots and Systems (IROS)*, 561–566.